Electronic Supporting Information for

Zeolite supramolecular framework with LTA based on tetrahedral metal-organic cage

Hai-Xia Zhang,‡[a] Xiaodong Yan,‡[a] Yu-Xin Chen,[a] Shu-Heng Zhang,[a] Tao Li,[a] Wang-Kang Han,[a] Ling-Yu Bao,[a] Rui Shen,[a] and Zhi-Guo Gu*[a,b]

[a] *Key Laboratory of Synthetic and Biological Colloids, Ministry of Education, School of Chemical and Material Engineering, Jiangnan University, Wuxi 214122, P.R.China.*
[b] *International Joint Research Center for Photoresponsive Molecules and Materials, School of Chemical and Material Engineering, Jiangnan University, Wuxi 214122, P.R. China.*

E-mail: zhiguogu@jiangnan.edu.cn

Table of contents

1. Experimental section

All reagents and solvents were reagent grade, purchased from commercial sources and used without further purification.

Caution: Although no problems were encountered in this work, the perchlorate salt was potentially explosive. Thus, this starting material should be handled in small quantities and with great caution!

Infrared spectra were measured on an ABB Bomem FTLA 2000-104 spectrometer with KBr pellets in the 500-4000 cm^{-1} region. NMR spectra were recorded on AVANCE III (400 MHz) instrument at 298 K using standard Varian or Bruker software, and chemical shifts were reported in parts per milion (ppm) downfield from tetramethylsilane. Element analyses were conducted on elementar corporation vario EL III analyzer. UV-Vis absorbance spectra were collected on Shimadzu UV-2101 PC scanning spectrophotometer. Solid UV-Vis spectra were collected on Shimadzu UV-3600 plus scanning spectrophotometer. Thermal gravimetric analysis (TGA) were carried out on a Waters TGA Q500 by heating the samples from 25 to 500°C under nitrogen atmosphere at a heating rate of 15 °C/min. VHX-1000C super deep scene 3D microscope with magnification 250-2500 times. Variable-temperature magnetic susceptibility on polycrystalline samples was performed on a Quantum Design MPMS-XL-7 SQUID magnetometer over the temperature range 2-400 K at 1000 Oe. The molar susceptibility was corrected for diamagnetic contributions using Pascal's constants and the increment method. Samples were restrained with petroleum jelly to prevent decomposing of the crystallites. All the encapsulated compounds used for the magnetic susceptibility measurement were the solution loading samples. High-resolution mass spectra (HRMS) were obtained on a Quadrupole-time-of-flight (Q-TOF) mass spectrometer and the fragment voltage was set at 175 V. The Raman spectra of the samples deposited on a glass slide were obtained from Invia Raman spectra (Reinshaw England) with 785 nm excitation line. Power X-ray Diffraction (PXRD) data on the crystalline were collected on a D8 Advance X-ray diffractometer (Bruker AXS Germany) with Cu Kα radiation in a 2θ range from 3° to 50° at the speed of 2°/min at room temperature. Low-pressure (up to 1 bar) gas adsorption isotherms (N_2) were

measured on a Micrometrics ASAP 2020 MP Surface Area and Porosity Analyzer. Regrettably, the Brunauer-Emmett-Teller (BET) surface area of **1** was only 8.6m^2/g maybe due to the high test pressure, which caused the flexible framework to become tightly packed.

2. Synthesis of 3,5-di(2-(1-(imidazole-2-carboxaldehyde)methyl))toluene

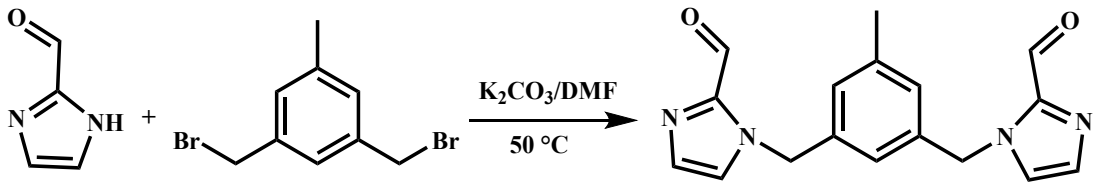

Imidazole-2-carboxaldehyde (2.12 g, 22 mmol), 3,5-di(bromomethyl)toluene (2.78 g, 10 mmol), and potassium carbonate (3.04 g, 22 mmol) were suspended in 50 mL DMF under nitrogen atmosphere. After stirring for 3 days at 50 °C, the reaction mixture was filtered. The filtrate was extracted with ethyl acetate (3 × 50 mL), collecting the organic phase, washed with saturated aqueous solution of potassium chloride, dried with anhydrous magnesium sulfate, removed the solvent on a rotary evaporator and dried under vacuum in 40 °C to give the desired product as yellow solids (Yield: 50.32 %). Pure light yellow crystals of 3,5-di(imidazole-2-carboxaldehyde)toluene were obtained by recrystallizing the crude product from ethyl acetate. Anal.Calcd for $C_{17}H_{16}N_4O_2$: C, 66.22; H, 5.23; N, 18.17. Found: C, 66.01; H, 5.35; N, 18.12. IR (KBr, νcm^{-1}, Fig. S1): 3087, 3016, 2972, 2925, 2852, 2740, 1683, 1604, 1473, 1411, 1336, 1299, 1274, 1224, 1155, 1074, 977, 914, 869, 813, 757, 692, 576. ^{1}H NMR (400 MHz, CD_3CN, δ ppm, Fig. S2): 9.72 (s, $2H^1$), 7.36 (s, $2H^2$), 7.28(s, $2H^3$), 6.96 (s, $2H^5$), 6.80 (s, $1H^7$), 5.54 (s, $4H^4$), 2.27(s, $3H^6$). ^{13}C NMR (400 MHz: CD_3CN, δ ppm, Fig. S3): 182.03, 143.34, 139.34, 137.75, 131.58, 127.40, 127.12, 123.17, 50.06, 20.10.

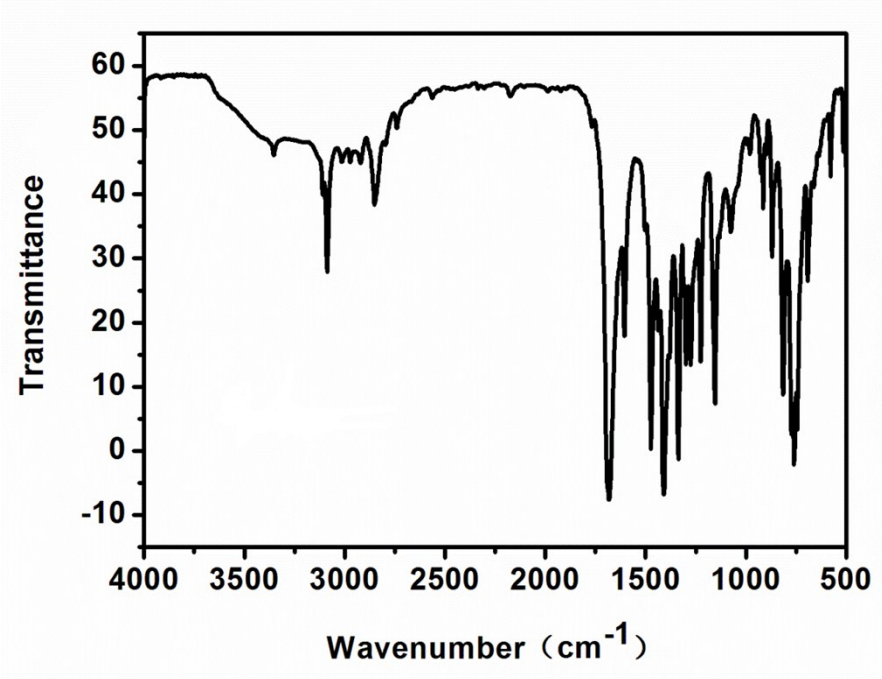

Fig. S1 IR spectrum of 3,5-di(imidazole-2-carboxaldehyde)toluene.

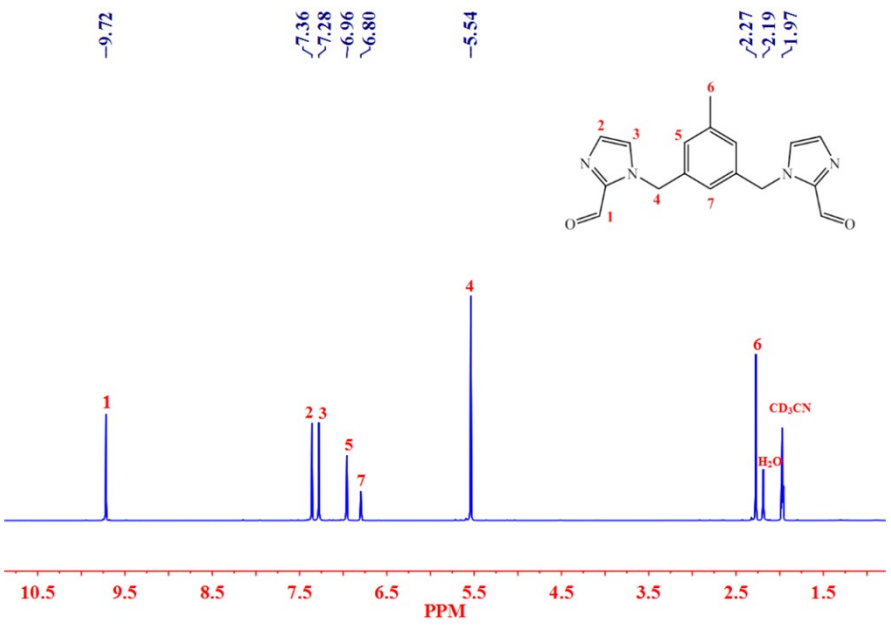

Fig. S2 ^{1}H NMR spectrum of 3,5-di(imidazole-2-carboxaldehyde)toluene.

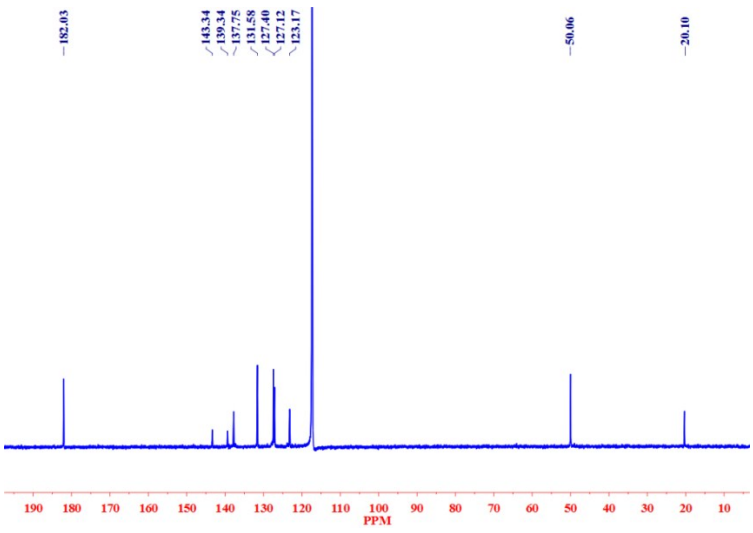

Fig. S3 ^{13}C NMR spectrum of 3,5-di(imidazole-2-carboxaldehyde)toluene.

3. Synthesis of 1

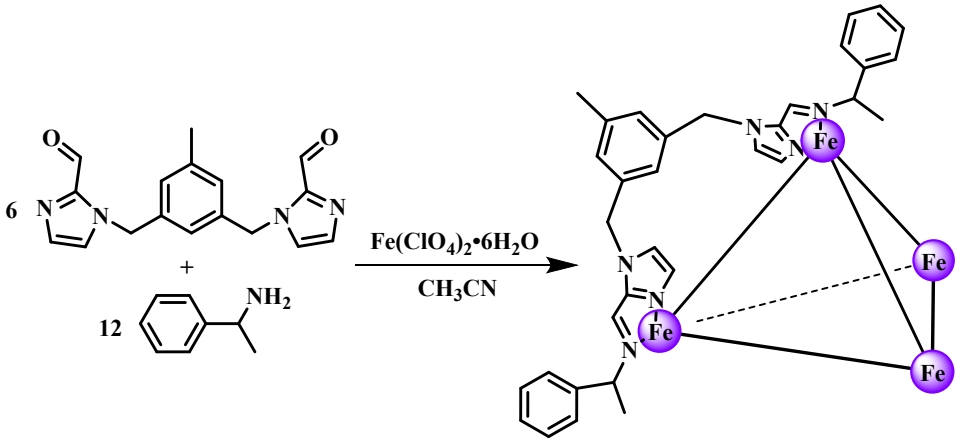

A solution of 3,5-di(2-(1-(imidazole-2-carboxaldehyde))methyl)toluene (61.67 mg, 0.2 mmol), (*R*)-1-phenylethylamine (48.47 mg, 0.4 mmol) and $Fe(ClO_4)_2 \cdot 6H_2O$ (48.4 mg, 0.13 mmol) in acetonitrile (20 mL) under nitrogen atmosphere. The solution was heated to reflux for 2 h at 80°C, and then cooled to room temperature. The resulting purple solution was filtered. **1** was precipitated as dark purple crystals through slow diffusion of diethyl ether into the filtrate at room temperature. Yield: 60.01 %. Anal. Calcd for $C_{198}H_{204}Fe_4Cl_8O_{32}N_{36}$: C, 57.90; H, 5.00; N, 12.28; Found: C, 58.16; H, 5.21; N, 12.11. IR (KBr, vcm^{-1}, Fig. S5): 3135, 2981, 2923, 1607, 1571, 1531, 1486, 1444, 1382, 1287, 1097, 964, 917, 844, 748, 700, 619. ^{1}H NMR (400 MHz, CD_3CN, δ ppm, Fig. S6): 14.08 (s, $2H^6$), 10.87 (s, $2H^7$), 10.65 (s, $2H^8$), 7.47-7.15 (m, $10H^{1-3}$), 6.52 (s,

3H[10,12]), 5.86 (d, 4H[9]), 4.95 (m, 2H[4]), 2.42-2.19 (m, 9H[5,11]). HR-MS (m/z, Fig. S7): [**1**$(ClO_4)_7$]$^+$ 4007.63, [**1**$(ClO_4)_6$]$^{2+}$ 1954.09, [**1**$(ClO_4)_5$]$^{3+}$ 1269.58, [**1**$(ClO_4)_4$]$^{4+}$ 927.32, [**1**$(ClO_4)_3$]$^{5+}$ 721.97, [**1**$(ClO_4)_2$]$^{6+}$ 585.06, [**1**(ClO_4)]$^{7+}$ 487.28, **1**$^{8+}$ 413.94.

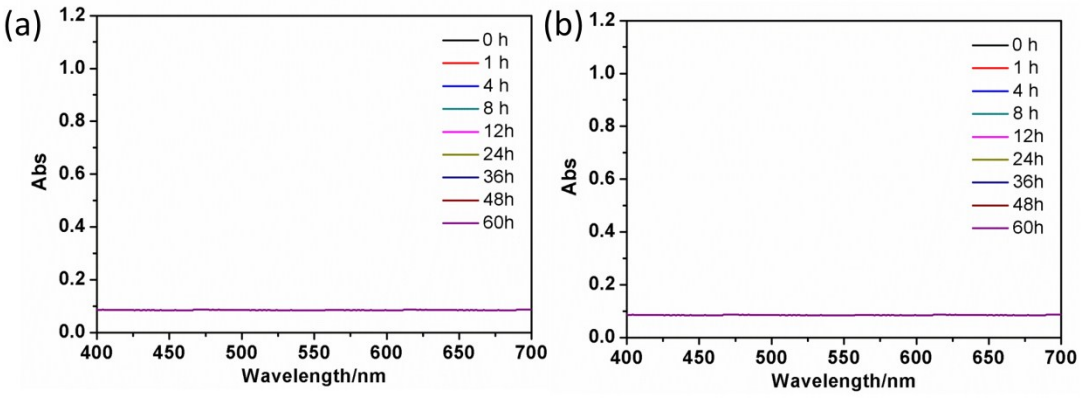

Fig. S4 The UV-vis spectra of **1** in the solvent. (a) n-hexane, (b) water.

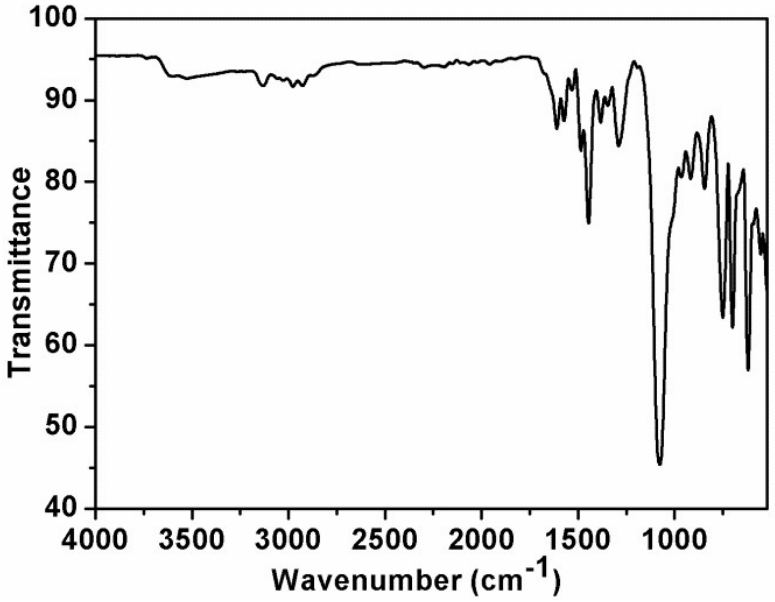

Fig. S5 IR spectrum of **1**.

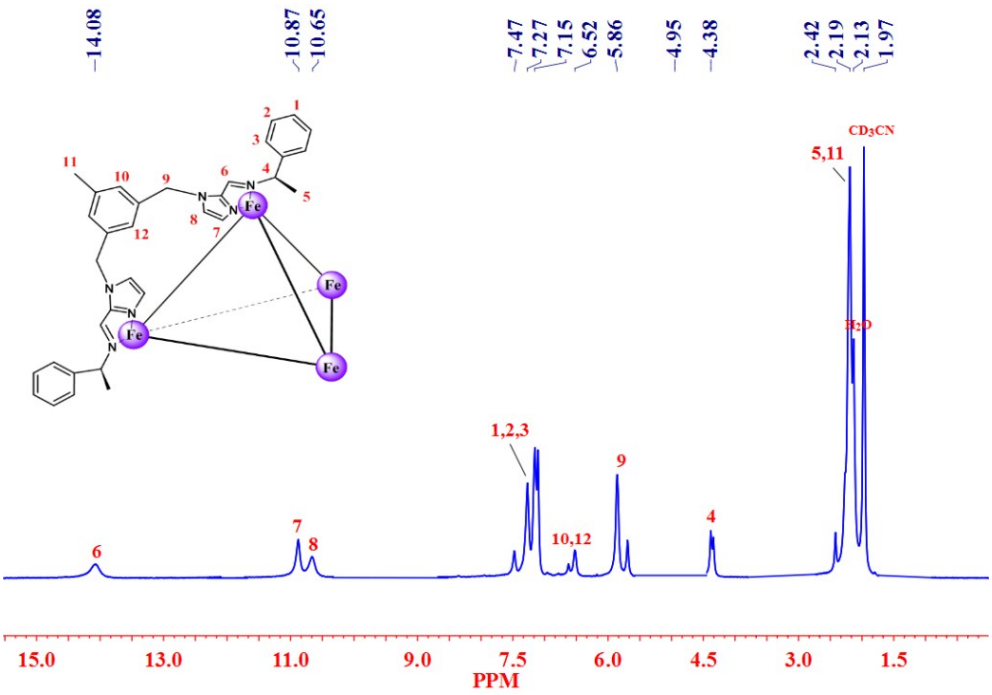

Fig. S6 ^{1}H NMR spectrum of **1**.

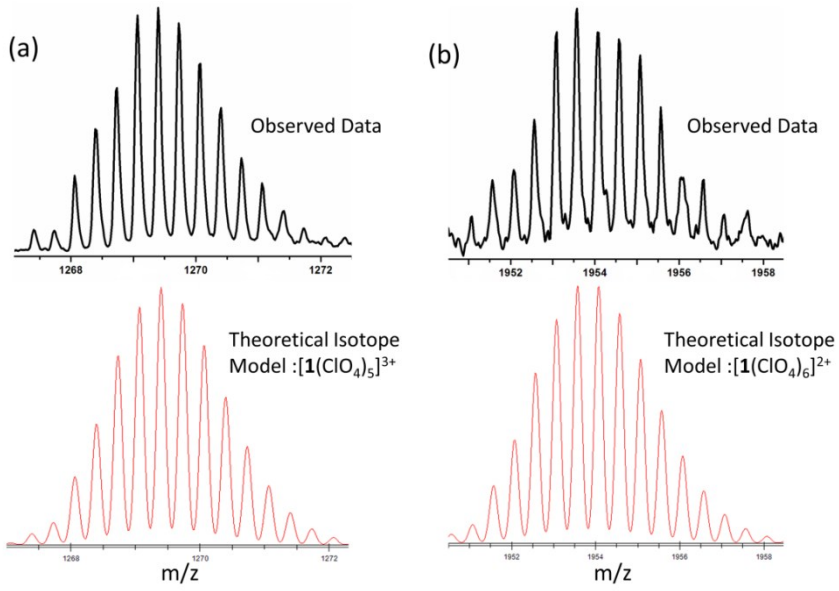

Fig. S7 High-resolution HR-MS spectra of **1** from an acetonitrile solution. Charges states from Z=2+ to 3+ are visible, each showing the sequential loss of a perchlorate counterion. (a) High resolution HR-MS and theoretical isotope modelof $[\mathbf{1}(ClO_4)_5]^{3+}$. (b) High resolution HR-MS and theoretical isotope model of $[\mathbf{1}(ClO_4)_6]^{2+}$.

4. Thermal stability of 1

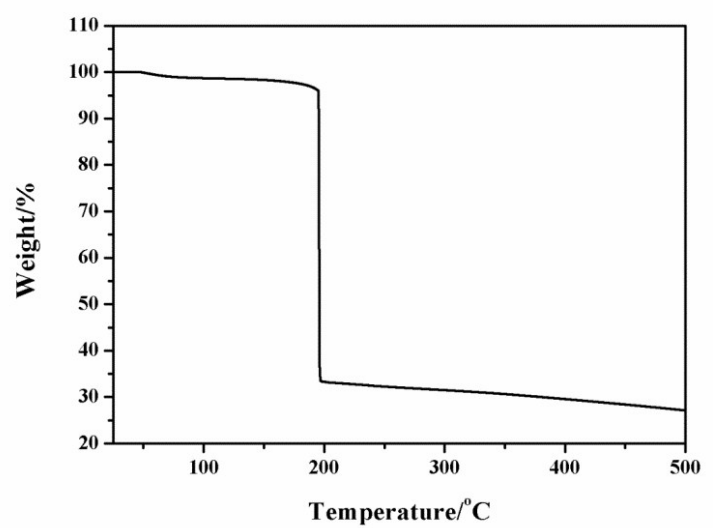

Fig. S8 TGA of profile of **1** crystals.

TGA under nitrogen showed a weight loss of 4.11 % below 195 °C（Fig. S8），corresponding to the release of water and solvent molecules of crystallization. The ClO_4^- ions exploded when the temperature at 195 °C, causing a sudden loss of the mass of the sample **1**.

5. The powder XRD pattern

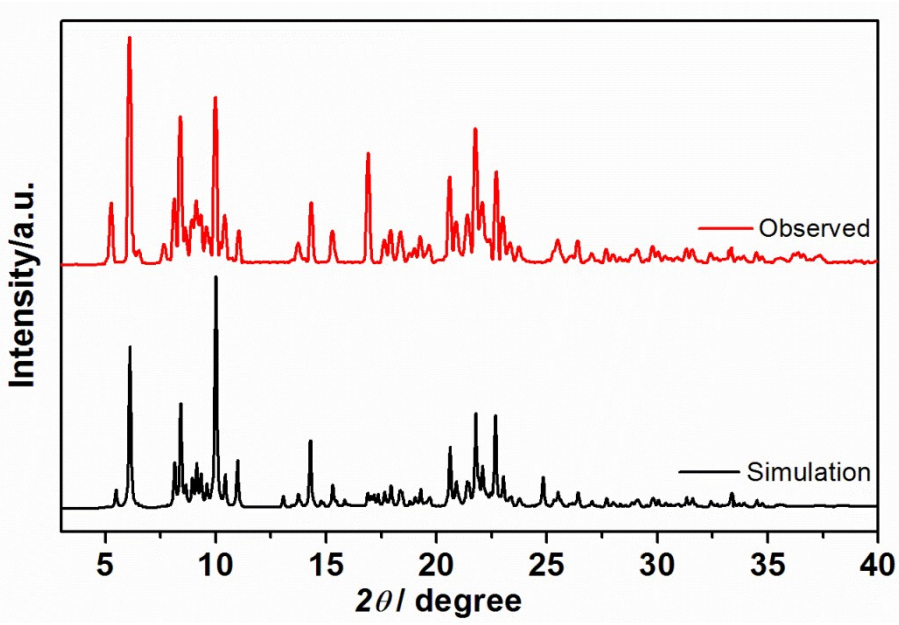

Fig. S9 Observed and simulated powder X-ray diffraction (PXRD) of **1**.

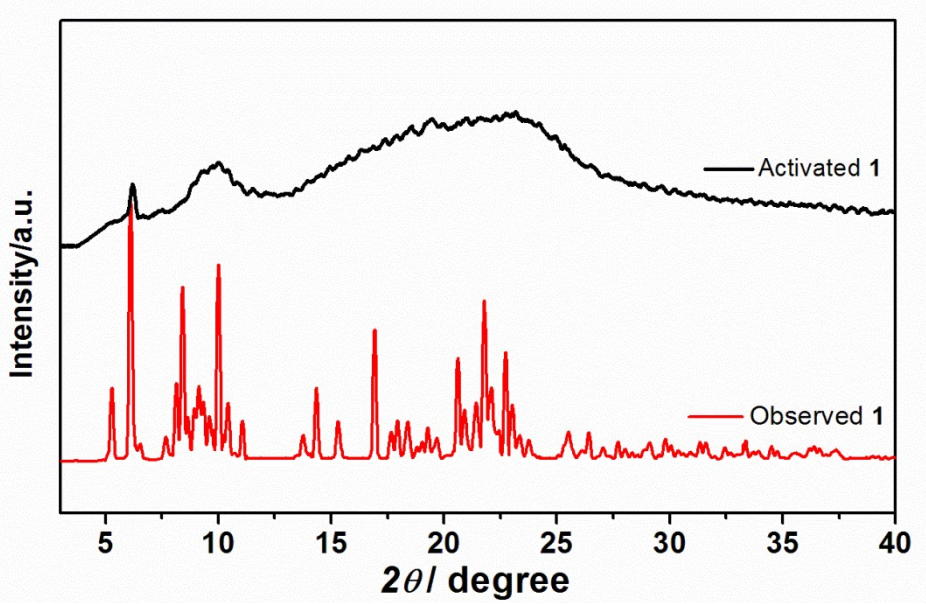

Fig. S10 Activated **1** (after BET test) and observed **1** powder X-ray diffraction (PXRD).

6. X-ray crystallographic data

The crystal structure were determined on a Siemens (Bruker) SMART CCD diffractometer using monochromated Mo $K\alpha$ radiation (λ = 0.71073 Å). Cell parameters were retrieved using SMART software and refined using SAINT[1] on all observed reflections. The highly redundant data sets were reduced using SAINT[1] and corrected for Lorentz and polarization effects. Absorption corrections were applied using SADABS[2] supplied by Bruker. Structure was solved by direct methods using the program SHELXL-97[3]. All of the non-hydrogen atoms except the anions were refined with anisotropic thermal displacement coefficients. Hydrogen atoms of organic ligands were located geometrically and refined in a riding model. Disorder was modeled using standard crystallographic methods including constraints, restraints and rigid bodies where necessary. The crystals of **1** decayed rapidly out of solvent, despite rapid handling and long exposure time, the data collected are less than ideal quality. The diffraction of the crystal was very weak. No diffraction was observed past 0.94 Å although the explosure time was increased to 100s per degree, and the data was trimmed. Reflecting the instability of the crystals, there is a large area of smeared electron density present in the lattice. Despite many attempts to model this region of disorder as a combination of solvent molecules no reasonable fit could be found and

accordingly this region was treated with the SQUEEZE[4] function of PLATON[5]. The carbon atoms C15H, C15G, C16H in the 3,5-di(imidazole-2-carboxaldehyde)toluene were disordered. Table S1 lists the crystallographic parameters concerning data collection and structure refinements for **1** while relevant bond lengths and angles (°) were listed in Table S2.

Table S1 Summary of crystallographic data for **1**

	1
Formula	$C_{594}H_{612}Cl_{16}O_{64}Fe_{12}N_{108}$
Fw	11525.3
T (K)	173(2)
λ (Å)	0.71073
Crystal system	Cubic
Space group	*F23*
a (Å)	54.053(4)
b (Å)	54.053(4)
c (Å)	54.053(4)
α (°)	90
β (°)	90
γ (°)	90
V (Å^3)	157931(18)
Z	8
D_{calc} (Mg/m^3)	0.969
μ (mm^{-1})	0.325
F(000)	48224
θ (°)	3.08-23.25
Index ranges	-59 ≤h≤ 53 -59≤k≤ 50 -15 ≤l≤ 42
reflections collected	34865
GOF (F^2)	1.030
$R_1{}^a$,$wR_2{}^b$($I>2\sigma(I)$)	0.1504, 0.3522
$R_1{}^a$,$wR_2{}^b$(all data)	0.2604, 0.4014

$R_1{}^a = \Sigma||F_o| - |F_c||/\Sigma|F_o|$. $wR_2{}^b = [\Sigma w(F_o{}^2 - F_c{}^2)^2/\Sigma w(F_o{}^2)]^{1/2}$.

Table S2. Selected bond lengths [Å] and angles [°] for **1**

1			
Fe(1)-N(1A)	1.982(12)	Fe(2)-N(1B)	1.974(11)
Fe(1)-N(1C)	1.948(13)	Fe(2)-N(1D)	1.977(14)
Fe(1)-N(1G)	1.940(13)	Fe(2)-N(1E)	1.936(11)
Fe(1)-N(3A)	1.991(12)	Fe(2)-N(3B)	1.999(13)
Fe(1)-N(3G)	2.037(11)	Fe(2)-N(3D)	2.000(13)
Fe(1)-N(3C)	2.033(13)	Fe(2)-N(3E)	2.015(12)
N(1G)-Fe(1)-N(1C)	93.2(6)	N(1E)-Fe(2)-N(1B)	91.3(5)
N(1G)-Fe(1)-N(1A)	91.6(5)	N(1E)-Fe(2)-N(1D)#1	91.6(5)
N(1C)-Fe(1)-N(1A)	95.2(6)	N(1B)-Fe(2)-N(1D)#1	93.3(6)
N(1G)-Fe(1)-N(3A)	91.3(5)	N(1E)-Fe(2)-N(3D)#1	171.8(5)
N(1C)-Fe(1)-N(3A)	173.1(5)	N(1B)-Fe(2)-N(3D)#1	93.7(5)
N(1A)-Fe(1)-N(3A)	79.4(5)	N(1D)#1-Fe(2)-N(3D)#1	81.6(6)
N(1G)-Fe(1)-N(3C)	172.7(5)	N(1E)-Fe(2)-N(3B)	92.6(5)
N(1C)-Fe(1)-N(3C)	80.5(6)	N(1B)-Fe(2)-N(3B)	81.1(5)
N(1A)-Fe(1)-N(3C)	92.5(5)	N(1D)#1-Fe(2)-N(3B)	173.0(6)
N(3A)-Fe(1)-N(3C)	95.3(5)	N(3D)#1-Fe(2)-N(3B)	94.5(5)
N(1G)-Fe(1)-N(3G)	81.1(5)	N(1E)-Fe(2)-N(3E)	79.3(6)
N(1C)-Fe(1)-N(3G)	91.7(5)	N(1B)-Fe(2)-N(3E)	169.5(5)
N(1A)-Fe(1)-N(3G)	170.3(5)	N(1D)#1-Fe(2)-N(3E)	91.8(6)
N(3A)-Fe(1)-N(3G)	94.2(5)	N(3D)#1-Fe(2)-N(3E)	96.1(5)
N(3C)-Fe(1)-N(3G)	95.3(5)	N(3B)-Fe(2)-N(3E)	94.5(5)

Symmetry transformations used to generate equivalent atoms: #1 x,-y,-z

7. The interactions in 1

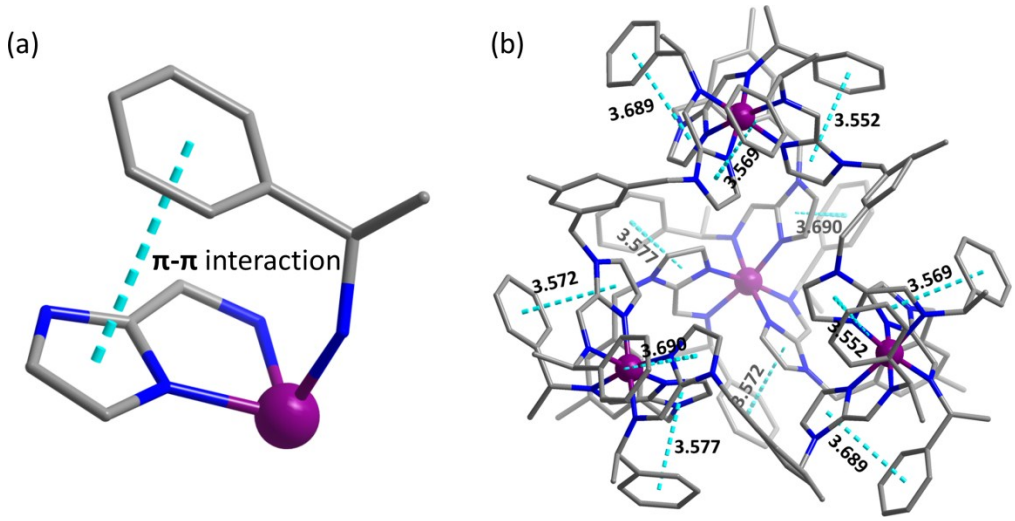

Fig. S11 (a) The diagram of intramolecular π-π interaction (turquoise dashed lines), (b) Intramolecular π-π interactions of **1**. All H atoms and lattice perchlorate anions have been removed for clarity (Fe: purple, C: gray, N: blue).

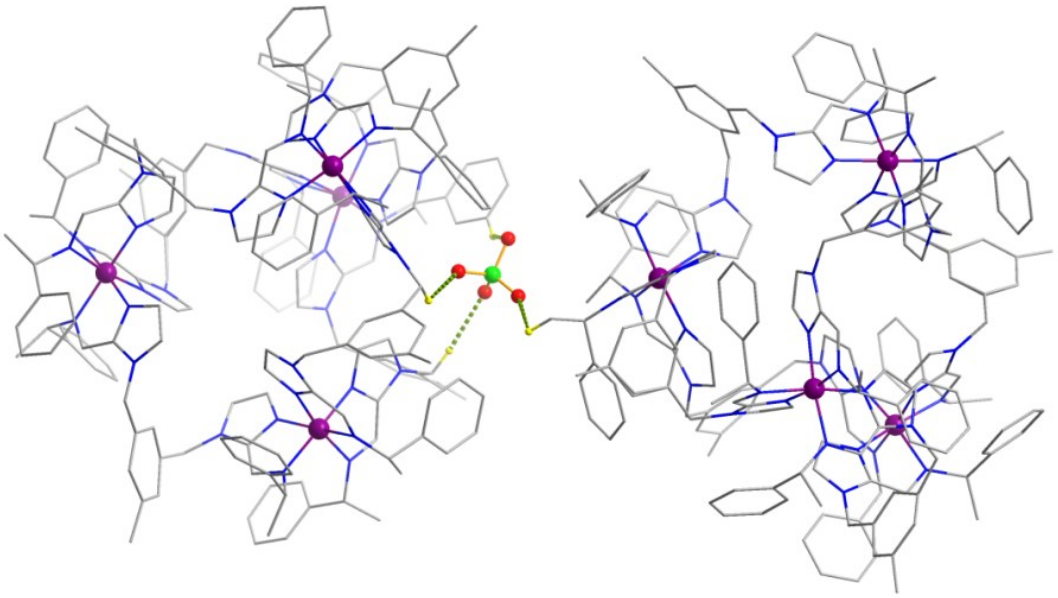

Fig. S12 The diagram of intramolecular hydrogen bond interactions (indicated by lime dashed lines; Fe: purple, C: gray, N: blue, O: red, Cl: green, H: yellow).

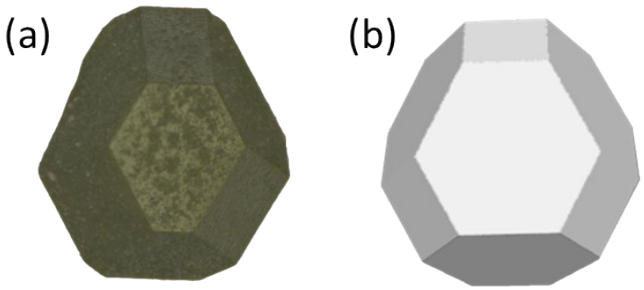

Fig. S13 (a) The photograph of one single crystal of **1** by super deep scene 3D microscope, (b) truncated octahedron.

8. Crystal packing diagram of 1

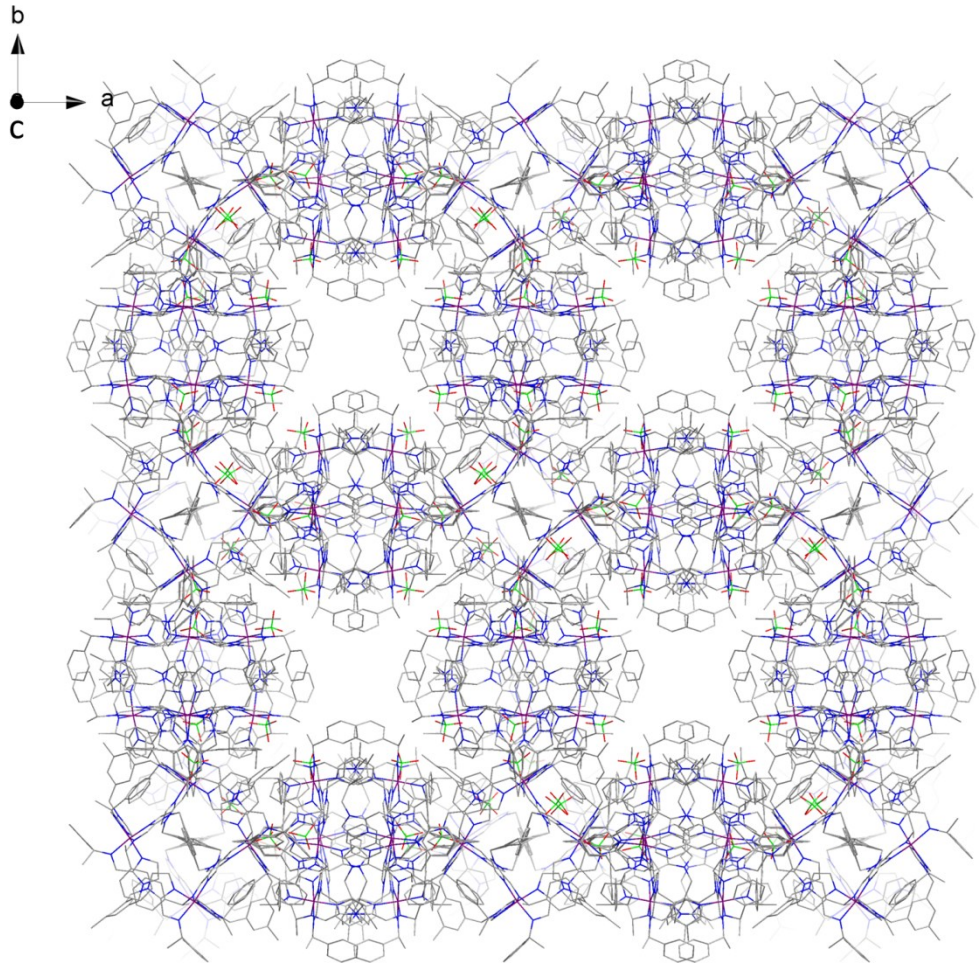

Fig. S14 Crystal packing diagram of **1**, viewed along c axis. All H atoms have been removed for clarity.

9. Experiment procedure for the uptake of iodine in solution phase

In order to monitor the iodine uptake of **1** in solution, a time-dependent UV-Vis measurement was carried out. The iodine solution was poured back to the original system after each measurement to keep invariability for total volume of sample solution. The crystals of **1** (20.0 mg) was added to an iodine solution (2.0 mmol L^{-1}, 8 mL). Then the amount of iodine captured by **1** can be calculated through subtracting the amount of iodine remained in solution from the initial amount of iodine. When **1** was immersed in a hexane solution of iodine in a small sealed vial at ambient temperature, the purple solution was found to fade slowly and became colorless 60 hours later. The residual iodine content were obtained by iodine concentration standard curve of absorbance, which were prepared by measuring absorbance of different determined concentrations of iodine solution at λmax 522 nm using a UV-Vis spectrophotometer.

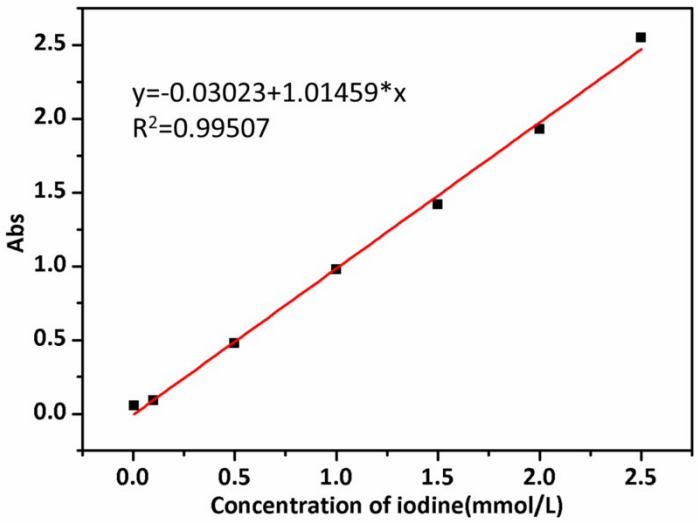

Fig. S15 Iodine concentration standard curve of absorbance.

10. Experiment procedure for iodine vapor uptake

Iodine vapor uptake experiment was performed in the following procedure: 10 mg of **1** crystals in an open glass bottle (1 mL) and excess iodine was placed in a sealed glass bottle (10 mL), heated at 75 °C and under ambient pressure in a drying oven. Put the glass bottle in the drying oven to make sure that each part of the glass bottle was

the same temperature, which avoided temperature gradient that may lead to iodine condensation on the surface of **1** crystals powder. After adsorption of the iodine vapor over time, the sample was cooled down to room temperature and weighed. Calculated the iodine uptake of **1** crystals powder by weight increase: $\alpha = \left[\frac{m2 - m1}{m1}\right] \times 100\ wt\%$, where α was the iodine adsorption, m_1 and m_2 were the mass of **1** crystal sample before and after being exposed to iodine vapor, respectively. The iodine uptake experiment was carried out four times and a good repeatability was observed.

11. Experiment procedure for dyes molecules uptake

Uptake experiments were implemented by immersing **1** in the aqueous solution of the dyes (Fig. S16) at room temperature. The UV-Vis spectrum of the solution was recorded periodically, and the solution was poured back to the original system after each measurement to keep invariability for total volume of sample solution. 15.0 mg of **1** was added to a 5 mL aqueous solution of dyes ([AM] = 60 μmol/L, [CR] = 120 μmol/L, [NR] = 40 μmol/L, [MB] = 12.6 μmol/L), which was put in 10 ml bottle. Then removed the supernatant and performed the UV-Vis spectrum measurement at different time during the entire adsorption process. After measuring, we removed back the solution to the original mixture to avoid the loss of samples. The absorbance at maximum wavelength (AM: λ_{max} = 522 nm, CR: λ_{max} = 529 nm) was selected to calculate the dye content, and the maximal adsorption capacity of dye was obtained by the corresponding dye concentration standard curve of absorbance (Fig. S17).

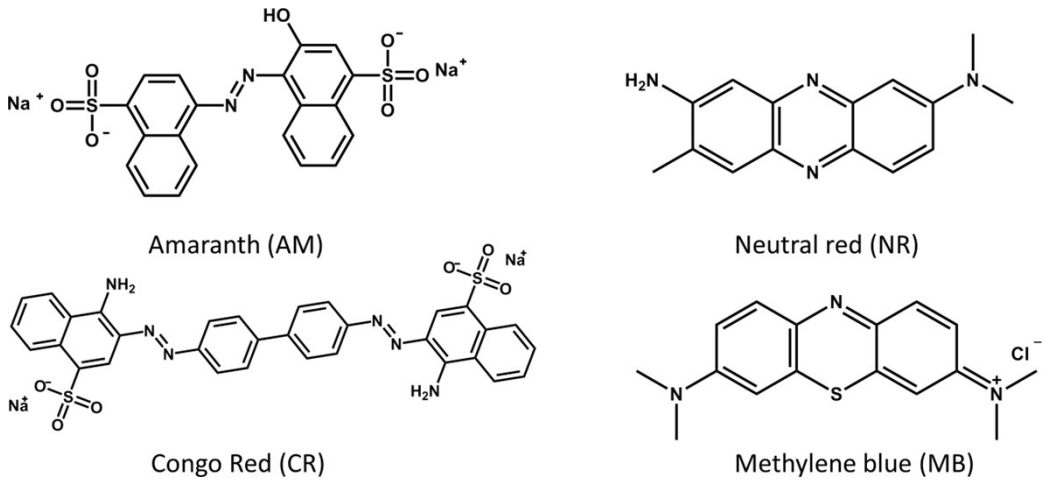

Fig. S16 Structures of guest dye molecules used in this study.

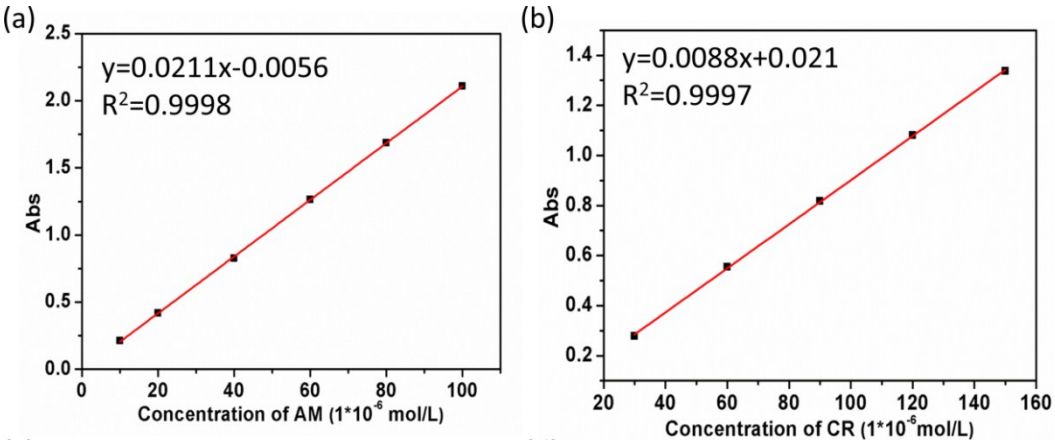

Fig. S17 Dye concentration standard curve of absorbance. (a) AM, (b) CR.

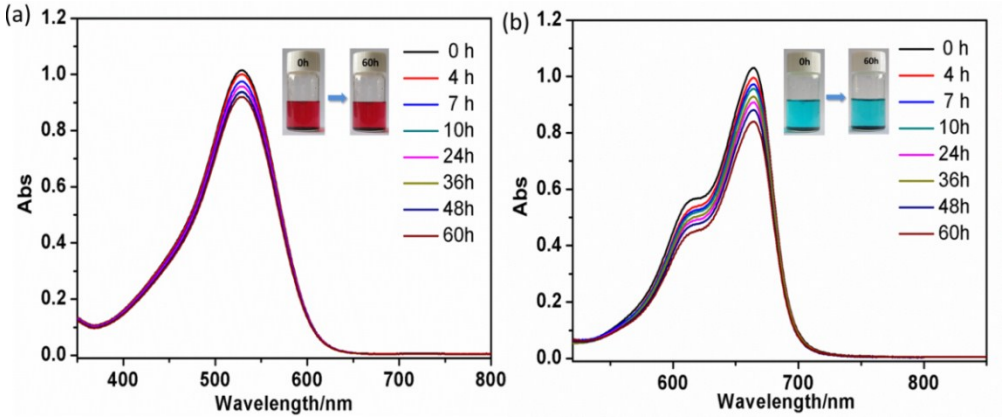

Fig. S18 (a) Time-dependent UV/Vis absorption spectra of the neutral red aqueous solution (NR, 5 mL, [NR] = 40 μmol/L) upon addition of 1 (15 mg). (b) Time-dependent UV/Vis absorption spectra of the methylene blue aqueous solution (MB, 5 mL, [MB] = 12.6 μmol/L) upon addition of 1 (15 mg). The photographs of bottles (insets) show the color of iodine and dyes molecules before and after inclusion.

12. IR spectra

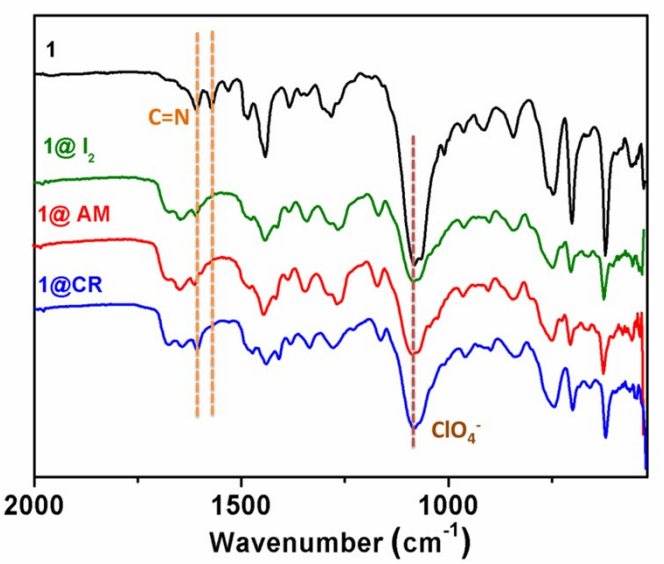

Fig. S19 IR spectra of **1**, **1@I_2**, **1@AM** and **1@CR**.

The typical absorptions for stretching of imidazole-imine (C=N) groups shifted to low wave numbers after iodine or dye molecules were encapsulated in the crystals **1**, which indirectly revealed the conversion of LS to HS in Fe(II) centers at room temperature.

13. Raman spectra

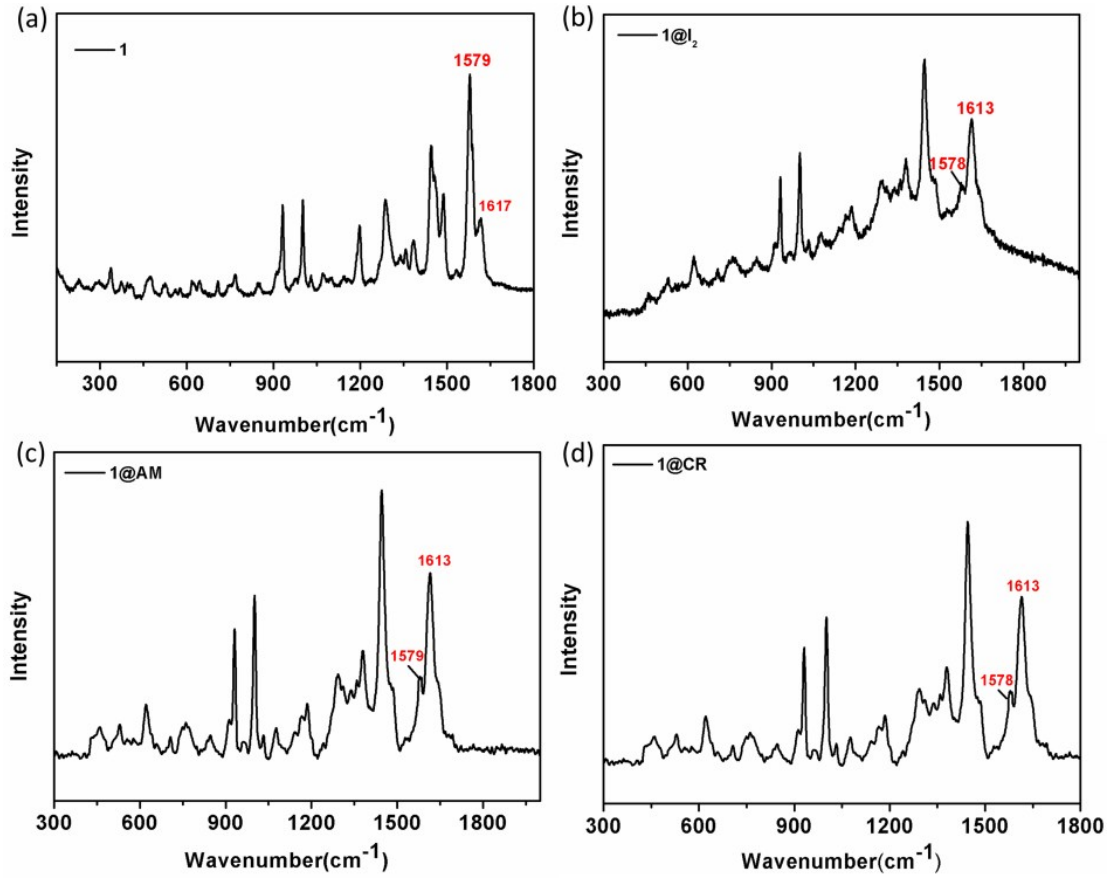

Fig. S20 Raman spectra of (a) **1**, (b) **1@I_2**, (c) **1@AM** and (d) **1@CR**.

The typical absorptions of imidazole-imine (C=N) groups in Raman spectra at 1579 cm^{-1} and 1617 cm^{-1}. After iodine and dyes were encapsulated in **1**, the peak intensity of C=N group at 1617 cm^{-1} weakened and shifted to low wave numbers 1613 cm^{-1}, the peak intensity of C=N group at 1579 cm^{-1} increased. This phenomenon indicated the spin state of Fe(II) centers transformed from LS to HS state.

14. Solid UV-Vis spectra

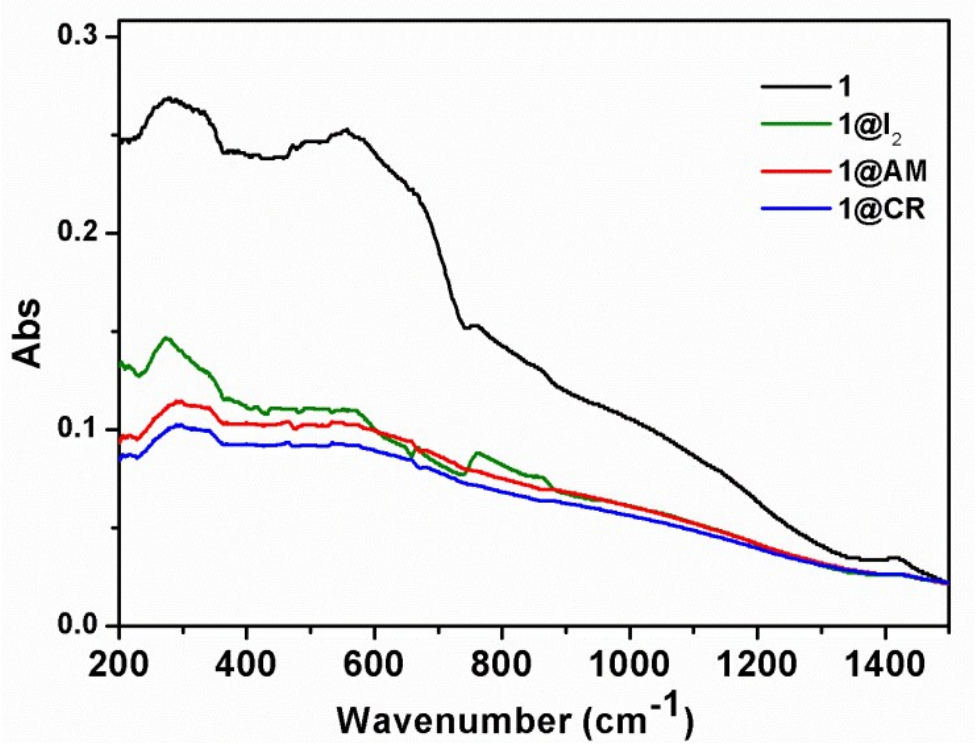

Fig. S21 Solid UV-Vis spectra of **1**, **1@I_2**, **1@AM** and **1@CR**.

The solid UV-Vis spectra of **1** exhibited metal-to-ligand charge transfer (MLCT) with characteristic broad bands at 556 nm, which indicated the low-state of **1** at room temperature. After adsorption of the guest molecules of iodine and the dyes of AM and CR, the intensity of MLCT peak decreased significantly, indicating the spin state of Fe(II) centers transformed from LS to HS state.

15. References

[1] *SAINT-Plus*, version 6.02; Bruker Analytical X-ray System: Madison, WI, 1999.

[2] G. M. Sheldrick, *SADABS An empirical absorption correction program*, Bruker Analytical X-ray Systems: Madison, WI, 1996.

[3] G. M. Sheldrick, *SHELXTL-97*; Universität of Göttingen: Göttingen, Germany, 1997.

[4] P. van der Sluis and A. L. Spek, *Acta Crystallogr., Sect. A: Found. Crystallogr.*, 1990, **46**, 194-201.

[5] A. Spek, *Acta Crystallogr., Sect. D: Biol. Crystallogr.*, 2009, **65**, 148-155.